Investigation of the Oxidation Zone in a Biomass two-stage downdraft Gasifier

Luc Gerun[*a], Jérôme Bellettre and Mohand Tazerout
Ecole des Mines de Nantes, DSEE
4, rue Alfred Kastler, B.P. 20722,
44 307 NANTES Cedex 3, France

Benny Gøbel[*b] and Ulrik Henriksen
Biomass Gasification Group,
Technical University of Denmark (DTU),
Forsøgsområde 120, Nordvej,
2800 Kongens Lyngby, Denmark

ABSTRACT

The partial combustion in a two-stage downdraft gasifier is critical for the process optimisation. Flame temperature and residence time of gas in the hot zone are indeed determining for tar cracking, the major issue in gasification. This paper presents a CFD model of the oxidation zone. Chemical reactions, including tar cracking, are treated by the "EDC" model (homogeneous reactions). Fluid flows are turbulent and simulated by the k-ε RNG turbulence model.
The validation of the model is done with the DTU 100 kW two-stage gasifier. Results fit satisfactory the data, regarding the temperature profile.
Keywords: Two-stage downdraft gasifier; partial oxidation; tar; modelling.

NOMENCLATURE

C	Concentration [kmol. m^{-3}]
c_p	Specific heat [J. kg^{-1}. K^{-1}]
d	Diameter [m]
$D_{0,r}$	Molar diffusion coefficient [kmol. m^{-3}]
E_a	Activation energy [J. $kmol^{-1}$]
h	Heat transfer coefficient [W. m^{-2}. K^{-1}]
h^0	Standard state enthalpy [J.kg^{-1}]
I	Radiative intensity [W. m^{-2}]
k	Thermal conductivity [W. m^{-2}. K^{-1}]
k_s	Frequency factor [s^{-1}]
k_c	Arrhenius kinetic rate [s^{-1}]
k_m	Mass diffusion coefficient [kg.m^{-2}.s^{-1}]
m	Mass [kg]
M	Molar weight [kg. $kmol^{-1}$]
n	Index of refraction
P	Pressure [Pa]
R	Ideal gas constant [8 314 J. $kmol^{-1}$]
$R_{i,r}$	Homogeneous reaction rate [kg. m^{-3}.s^{-1}]
T	Temperature [K]
u	Axial velocity [m.s^{-1}]
v	Radial velocity [m.s^{-1}]
x	Axial coordinate [m]
Y	Mass fraction, $Y_i = \frac{m_i}{m_{total}}$

Greek Letters

α	Absorption coefficient [m^{-1}]
α_{Pr}	Inverse of the turbulent Prandtl number
ε_m	Emissivity
ϕ	Hydraulic diameter [m]
ν	Kinematic viscosity [m². s^{-1}]
ρ	Density [kg. m^{-3}]
σ_S	Scattering coefficient [m^{-1}]
σ	Boltzman constant [5.67×10^{-8} W.m^{-2}.K^{-4}]

[*a] Corresponding author: E-mail: luc.gerun@emn.fr, phone number: (+33) 2 51 85 82 81, fax (+33) 2 51 85 82 99
[*b] Corresponding author: E-mail: bg@mek.dtu.dk , phone number: (+45) 45 25 41 74, fax (+45) 45 93 57 61

INTRODUCTION

The energy crisis of the 1970s sparked a renewed interest in biomass gasification systems. Nowadays environmental concerns are questioning the continued use of fossil fuels and the need for sustainable energy production has prompted new research into the possibility of gasification as a key source of energy production.
Gasification is a thermal process converting biomass feedstock into a mixture of gases that can be burnt in boilers, internal combustion engines and gas turbines.
If well designed, gasification allows an environmentally friendly energy production. Furthermore, it can help reducing the "waste disposal" constraints by using it as a feedstock to convert it into useful and valued product.
Biomass is indeed a particular kind of fuel. Its price is fixed by the collecting expenses. That is why small-scale installations are well adapted to this market. They allow valorising wastes directly on their production location.
In these perspectives downdraft gasifiers present indisputable advantages [1]. A traditional example is presented in *Figure 1* [2]. In current pilots called two-stage, drying/pyrolysis and combustion/reduction zones are physically separated. This low tar level technology only requires a small gas-cleaning unit to prevent engine fouling problems [3]. Furthermore it is well adapted to turnover and biomass diversity. Finally its utilisation is relatively easy and can be highly automated.
However available kinetics data and the theoretical comprehension of the physical phenomena remain still insufficient to build a general accurate model.

This paper presents a tool for validating two-stage downdraft gasifier design. In this type of installation, temperature field in the partial oxidation zone is crucial. Indeed gas produced during pyrolysis must pass through a hot uniform zone to crack satisfactorily tar, the main issue of gasifier. As a result, reactor diameter, throat shape and nozzle geometry have to be well designed in order to ensure an optimum process.
A CFD model is used to simulate the complex phenomena occurring in the partial oxidation zone. It includes detailed chemical mechanism with tar cracking, heat transfer with radiation and turbulent fluid flow.

Vijeu's pyrolysis model [4] is used to determine input pyrolysis gas composition, given in *Table 1* at a temperature of 650°C.
Results are then validated with the experimental data get from the DTU 100 kW_{th} two-stage gasifier [5,6]. They are finally discussed.

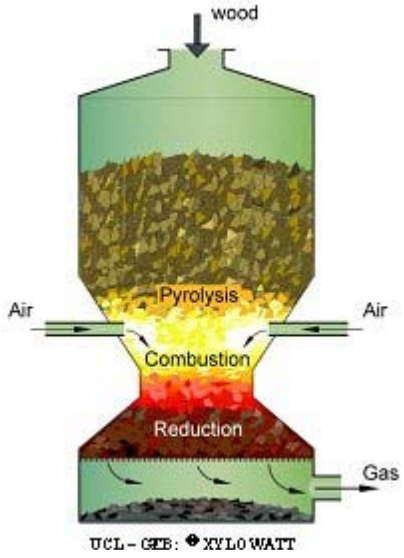

Figure 1: *Traditional downdraft gasifier [2]*

CO	CO_2	H_2	H_2O	CH_4	C_6H_6	$C_{10}H_8$
35[a]	20.8[a]	2.4[a]	7.2[a]	9.6[a]	8.7[b]	16.3[b]

a: calculated by Vijeu's pyrolysis model [4]
b: estimated [3,7]
Table 1: *Pyrolysis gas composition (mass %)*

MODEL

The model is divided into three parts: fluid flow, chemical mechanism and heat transfer. Model equations are listed in *Table 2*. *Figure 2* shows model geometry and boundary conditions.

Fluid flow

Air is injected into the reactor through three injectors with five nozzles each. Reynolds number is around 2,000 at the air injector nozzles. The flow may thus be turbulent in this zone. Moreover velocity pattern is complex as recirculation may occur.
A detailed turbulence model is thus required to simulate these phenomena. After a preliminary sensitivity study, the RNG k-ε model was chosen

Pyrolysis gas + steam inlet
u = 0.52 m/s, turbulence intensity: 3%, T=650°C, hydraulic diameter: ϕ =0.26 m.

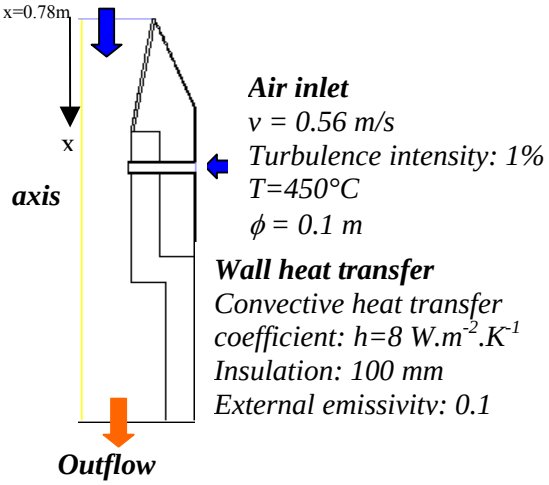

Figure 2: *Model geometry*

as the best compromise between accuracy and efficiency. It is also adequate for laminar flow that may develop inside the gasifier.
Wall boundary conditions are simulated by a low Reynolds number approach [8]. Solid phase is modelled by a Lagrangian particles tracking.

Chemical mechanism

The chemical mechanism consists in five oxidation reactions (1-5) and the water-gas shift reaction (6).

$$CO + 0.5\ O_2 \longrightarrow CO_2 \quad (1)$$
$$CH_4 + 1.5\ O_2 \longrightarrow CO + 2\ H_2O \quad (2)$$
$$H_2 + 0.5\ O_2 \longrightarrow H_2O \quad (3)$$
$$C_6H_6 + 4.5\ O_2 \longrightarrow 6\ CO + 3\ H_2O \quad (4)$$
$$C_{10}H_8 + 7\ O_2 \longrightarrow 10\ CO + 4\ H_2O \quad (5)$$
$$CO + H_2O \longleftrightarrow CO_2 + H_2 \quad (6)$$

Arrhenius rate is calculated from equation (7).

$$k_c = k_s e^{-\frac{E_a}{RT}} [A]^a [B]^b \quad (7)$$

Constants are taken from literature. They are listed in *Table 3*. The reverse term of (6) is obtained by a free Gibbs energy variation method.

Tars are modelled as a simplification of Jess works [9]. Pyrolysis, as it is slow and long, is considered to produce only secondary tar compounds, represented by benzene, and tertiary tar compounds, represented by naphthalene.
Naphthalene is indeed one of the main component of tar and 6C ring hydrocarbons are considered as the key component of thermal decomposition of aromatic hydrocarbon [9].
Further model development should include oxygenated hydrocarbons as phenol, whose concentration is not negligible particularly in steam gasification [10].
Initial tar concentration is extrapolated from literature data [3,7]. Methane includes C_2 compounds as ethane and ethylene. Tars are considered to be thermally cracked and to form soot. *Figure 2* shows the tar evolution mechanism. The kinetics constants of the five reactions are taken from Jess [9,11].

As flow is turbulent, it must be taken in consideration in the chemical reaction model. The chosen model, called "Eddy Dissipation Concept" model [12], calculates also Arrhenius rate at the turbulence time scale (18). It seems to suit well to this kind of reactive flow [13].

Besides it is observed that particles residence time is relatively short (<1s) in a two-stage downdraft gasifier. As a consequence heterogeneous reactions are negligible in the oxidation zone, as oxygen reacts far quicker with gas phase.

Heat transfer

As temperature exceeds 1000°C in the reactor core, heat transfer by radiation is predominant. They are simulated by the Discrete Ordinates model [14], a four-flux method. It integrates the Radiative Transfer Equation (13). As a result a source term S_f due to radiative transfer is included in the energy equation (12). S_f also includes the heat of the chemical reactions from equation (8).

$$S_{f,r} = -\sum_j \left(\frac{h_j^0}{M_j} + \int_{T_{ref,j}}^{T} c_{p,j} dT \right) R_{j,r} \quad (8)$$

The absorption coefficient of the fluid phase is computed by the cell-based Weighted-Sum-of-Gray-Gases model [15]. It only takes into account the concentration of CO_2 and H_2O.

Heat transfer from fluid to solid phase is calculated by equation (9).

$$m_p Cp_p \frac{dT_p}{dt} = hA_p\left(T_\infty - T_p\right) - \frac{dm_p}{dt} H_r + A_p \varepsilon_p \sigma (T_\infty^4 - T_p^4) \qquad (9)$$

Numerical solution

A segregated solver solves sequentially the continuity, momentum (Navier-Stokes equations), energy, radiation and species equations (N-1 equations for N species).

Governing equations are converted to algebraic equations that can be solved numerically by a control-volume-based technique through a power-law scheme [16]. SIMPLE algorithm couples velocity and pressure [17].

Simulation is 2D axisymmetric. In this purpose, the air injector, which is composed of five cylinders with three nozzles each, is considered as annular. Flowrate and injection surface area are conserved. Thus momentum is also conserved. Previous studies showed that this analogy was correct in this kind of problem [18].

However swirl neglecting may be a source of error.

The unstructured grid is composed of 20,000 cells. Meshing tests have been performed from 5,000 to 30,000 cells to insure independence of results.

Simulation is considered as converged when residuals remain constant at a value below 10^{-5} (10^{-4} for momentum). The calculation time is approximately fifty hours on a 3.2 GHz computer.

Mass $$\frac{\partial \rho}{\partial t} + \nabla.(\rho \vec{v}) = \mathrm{S_m} \qquad (10)$$

Momentum $$\frac{\partial}{\partial t}(\rho \vec{v}) + \nabla.(\rho \vec{v}\vec{v}) = -\nabla p + \nabla.(\bar{\bar{\tau}}) + \rho \vec{g} + \vec{F} \qquad (11)$$

Energy $$\frac{\partial}{\partial t}(\rho E) + \nabla.(\vec{v}(\rho E + p)) = \nabla.\left[k_{eff} \nabla T - (\sum_j h_h \vec{J}_j) + (\bar{\bar{\tau}}.\vec{v})\right] + S_f \qquad (12)$$

with $k_{eff} = \alpha_{\mathrm{Pr}} \mu_{eff} Cp$ [8]

Radiative transfer

$$\nabla.(I(\vec{r},\vec{s})\vec{s}) + (\alpha + \sigma_S) I(\vec{r},\vec{s}) = \alpha n^2 \frac{\sigma T^4}{\pi} + E_p + \frac{\sigma_S}{4\pi} \int_0^{4\pi} I(\vec{r},\vec{s}) \Phi(\vec{s}.\vec{s}') d\Omega' \ ) \qquad (13)$$

Turbulence $$\frac{\partial\left(\rho U_j k\right)}{\partial x_j} = \frac{\partial}{\partial x_j}\left[\rho \alpha_k \nu_{eff} \frac{\partial k}{\partial x_j}\right] + \rho \nu_t \left(\frac{\partial U_i}{\partial x_j} + \frac{\partial U_j}{\partial x_i}\right)\frac{\partial U_i}{\partial x_j} - \rho\varepsilon \qquad (14)$$

$$\frac{\partial\left(\rho U_j \varepsilon\right)}{\partial x_j} = \frac{\partial}{\partial x_j}\left(\rho \alpha_\varepsilon \nu_{eff} \frac{\partial \varepsilon}{\partial x_j}\right) + C_{\varepsilon 1} \frac{\varepsilon}{k} \rho \nu_t \left(\frac{\partial U_i}{\partial x_j} + \frac{\partial U_j}{\partial x_i}\right)\frac{\partial U_i}{\partial x_j} - C_{\varepsilon 2} \rho \frac{\varepsilon^2}{k} - R \qquad (15)$$

with $\nu_{eff} = \nu\left(1 + \sqrt{\frac{C_\mu}{\nu}} \frac{k}{\sqrt{\varepsilon}}\right)^2 = \nu\left(1 + \sqrt{\nu_t / \nu}\right)^2$

$C_\mu = 0.0845$; $C_{\varepsilon 1} = 1.42$ and $C_{\varepsilon 2} = 1.68$. α_k and α_ε are the inverse of turbulent Prandtl number for k and ε.

Species transport $$\frac{\partial}{\partial t}(\rho Y_i) + \nabla.(\rho \vec{v} Y_i) = -\nabla.\left(-\left(\rho D_{0,i} + \frac{\mu_t}{Sc_t}\right)\nabla Y_i\right) + R_i \qquad (16)$$

Homogeneous reaction rate $$R_{i,r} = \frac{(\xi^*)^2 \chi}{\tau^*}(Y_i^* - Y_i) \qquad (17)$$

With $\xi^* = C_\xi \left(\frac{\upsilon\varepsilon}{k^2}\right)^{\frac{3}{4}}$; $\tau^* = C_\tau \left(\frac{\upsilon}{\varepsilon}\right)^{\frac{1}{2}}$; $\chi = \frac{\rho}{[1 - (\xi^*)^3]}$; $C_\xi = 2{,}1377$; $C_\tau = 0{,}4082$.

Table 2: *Governing equations*

Reaction	k_s (s^{-1})	E_a (J. $kmol^{-1}$)	A	B	Reference
(1)	$1.3\times10^{11}\times[H_2O]^{0.5}$	1.256×10^{8}	1	0.5	Shin [19]
(2)	4.4×10^{11}	1.2552×10^{8}	0.5	1.25	Jones [20]
(3)	4.462×10^{12}	4.2×10^{7}	1	1	Di Blasi [21]
(4)	2.4×10^{11}	1.2552×10^{8}	1[a]	1.85	Westbrook [22]
(5)	$9.2\times10^{6}\times T$	8×10^{7}	0.5	1	Di Blasi [21]
(6)	124.03	1.26×10^{7}	1	1	Di Blasi [21]

a: modified (see Results &Discussion)

Table 3: *Reference value for kinetic constants*

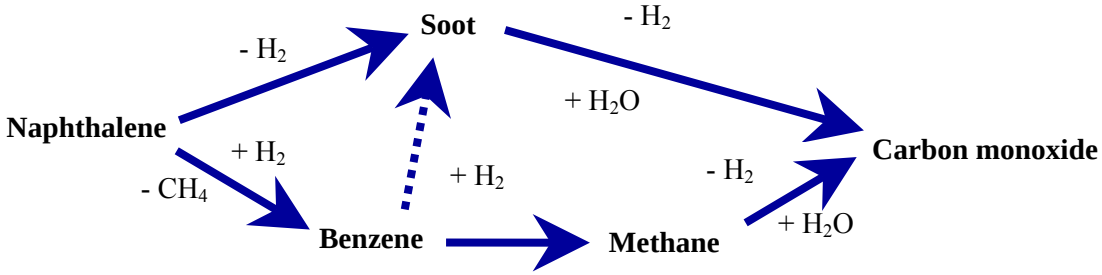

Figure 2: *Tar cracking mechanism*

EXPERIMENTAL

Facilities

The plant is a two-stage gasifier built at DTU with a thermal input of 100 kW. It consists of following components: propane heated pyrolysis unit, partial oxidation zone, air preheater, steam feeder and char bed lying on a movable grate [6]. It is showed in *Figure 3*.

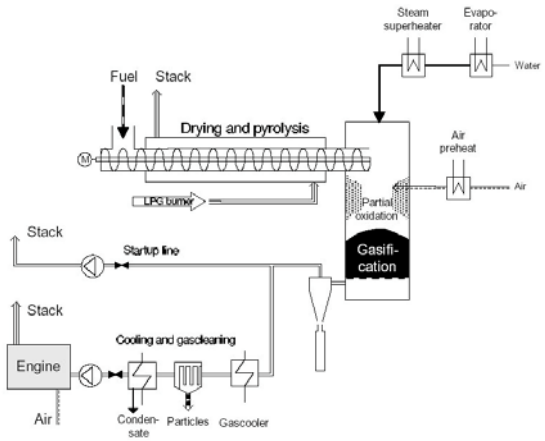

Figure 3: *100 kW_{th} two—stage gasifier*

Operating conditions

Experiments are performed with wood chips. Wood moisture is 26.5% of the total mass and the wood elementary formula is $CH_{1.4515}O_{0.66}$. Operating conditions are reported in *Table 4*.

	Wood	Air	Steam
Flowrate	24.8 kg/h	25 kg/h	7 kg/h
Initial temperature	600°C	≈450°C	600°C

Table 4: *Operating conditions*

Method of investigation

Temperature field inside the reactor was investigated through two different techniques.
A rod equipped with nine thermocouples measures the temperature along the vertical axis. It is movable and thus can inspect the radial temperature profile.
Secondly an infra red detector and a suction pyrometer are used to measure axial temperature in the symmetry axis.
Gas was analysed at the end of the process, i.e. after the reduction zone. Tar level is below 25 mg/Nm^3. The final dry gas composition is in volume-%: 17 CO, 17 CO_2, 2 CH_4 32 H_2 and 32 N_2. The soot particles concentration is around 450 mg/Nm^3 at the exit.

RESULTS & DISCUSSION

Temperature field

The *Figure 4* shows the comparison of the temperature profile along the vertical axis between the infrared measurement and the simulation

results. It fits satisfactorily the experimental data, although temperature is slightly overestimated. It may be partially due to an overestimation of the gas pyrolysis heating value.

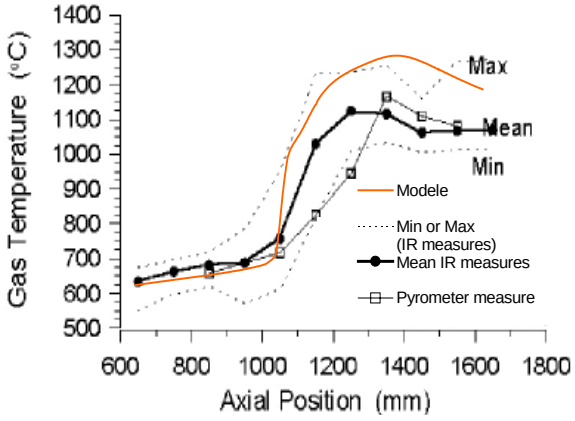

Figure 4: *Comparison modele/experiences results*

Temperature field is shown in *Figure 5*. The reaction heat is released mainly close to the injector. It induces a very hot zone in this area.

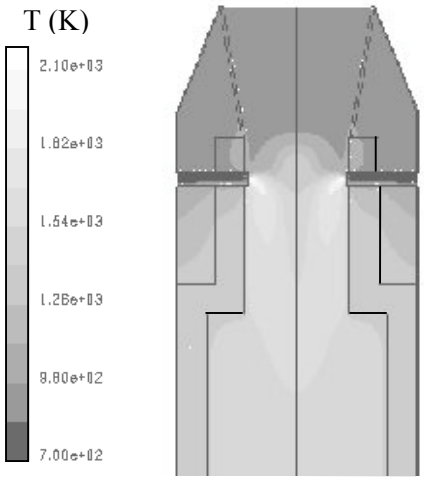

Figure 5: *Temperature field inside the reactor*

The uncertainties of measure and the operating conditions make the comparisons between experience and simulation difficult.
Indeed gasification is not a totally steady-state process. Inlet gas composition may for example vary strongly with time, as pyrolysis is also not fully stable. The effects of pyrolysis unsteadiness are studied later.

Flow pattern

The air velocity at the nozzle outlet is around 48 m/s, as the constriction accelerates the air. It implies fully developed turbulence in the flow and recirculations. These latter are shown in *Figure 6*.

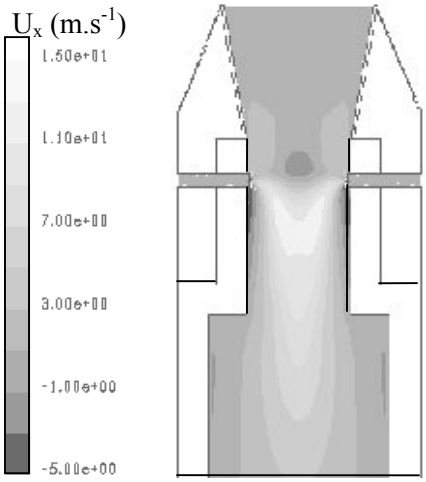

Figure 6: *Axial velocity inside the reactor*

Effect of the injection surface area

The injection surface area influences strongly the flow. Smaller nozzles induce higher air radial velocity but also higher axial gas velocity. As a result air penetrates deeper in the reactor, temperature is thus more uniform than with bigger nozzles. In the latter case the very hot zone located close to the wall is bigger. Temperature along the axis is shown in *Figure 7*.

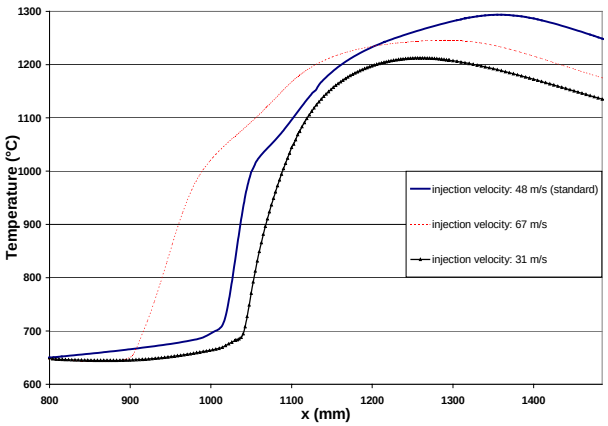

Figure 7: *Axial temperature with different nozzles*

The injector should also be carefully designed. A low opening area will induce better mixing and higher turbulence rate, necessary for a good combustion, but high gas velocity and thus smaller residence time too. This tool is also useful to find the best compromise to optimise the process.

Unsteady-state effects

The pyrolysis unsteady effects on temperature profile have been studied with the model. *Figure 8* shows a comparison of the axial temperature in the standard case, with 10% lower pyrolysis gas flowrate and with two different pyrolysis gas compositions – poorer and richer, respectively -/+ 20% [CO], [H_2], [CH_4], +/- the difference [CO_2].
It is observed that instabilities influence significantly the process. They should also be taken into account during a gasifier conception.

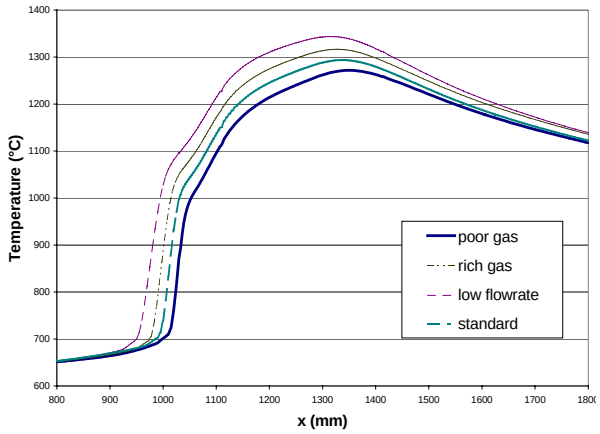

Figure 8: *Effect of pyrolysis unsteadiness on vertical axial temperature*

Chemical model discussion

The simulated final gas composition, summarised in *Table 5*, is in good agreement with experimental observations. Reduction reactions indeed convert water and char to hydrogen and carbon monoxide, diluting the mixture. Moreover the water-gas shift reaction, catalysed by the char bed, modifies the mixture composition.
It will be used in a future study as input for a reduction model to obtain a complete gasification model and then to compare numerical and experimental gas composition.

Conditions	CO	CO_2	H_2	CH_4	N_2
Standard	17.9	14.1	11.4	6.6	50
Poor gas	16.2	17.9	9.6	5.5	50.8
Rich gas	19.3	10.5	12.9	7.6	49.7
Low flowrate	16.9	13.9	10.1	6	53.1

Table 5: *Final gas dry composition (volume %)*

The modelling of competitive combustion reactions in an oxygen-limiting environment presents two main difficulties.
Firstly kinetic data are often determined for complete oxidation. Uniform sources have thus to be find or adaptations to be made.
That is why the –0.1 coefficient for benzene in its oxidation reaction (5) has been switched to 1. It implied furthermore heavy problems of solution convergence. Moreover the mechanism is very stiff and it is difficult to make it converged. It requires much time and precautions.
Besides the attempt of tar modelling is not a complete success. Naphthalene is reduced by a 5 factor during the process. It is far from the experimental results in similar case, which shows a decrease by a 100 factor. This difference can be partially explained by the neglecting of swirl effects. Residence time in simulation is thus lower than in reality.
The kinetic constants appear also to be uncertain. As already observed by Morf [10], naphthalene conversion to soot is negligible with rate of [5] used in this study. It means that either different pathways to produce soot exist or that the kinetic constants, calculated for coke-oven gas, are not adapted to biomass gasification.
To verify the later hypothesis, a try with a first order rate from Diesel combustion [23] has been performed. Naphthalene conversion to soot is then complete, whereas it was negligible with previous rate. Further kinetic study is thus required.

CONCLUSION

The oxidation zone of a two-stage downdraft gasifier has been simulated by a 2D CFD model. It takes into account turbulence, detailed chemical mechanism including tars and heat transfer.
Results fit satisfactorily to the experimental data regarding temperature pattern. However tar model requires further investigation.
Simulations enlightened several crucial point of the process:

- injector design is fundamental in gasification;
- pyrolysis unsteadiness influences significantly the process;
- kinetic data adapted to the process should be determined to ensure the tar model precision.

REFERENCES

[1] McKendry, P., *Energy production from biomass (part 3): gasification technologies*, Bioresource Technology 2002;83;55-63.

[2] Tchouate Heteu, P. M., *Feasibility of biomass gasification for decentralised rural electrification and industry in remote areas in Africa*, In: Proceedings of the First Int. Conf. and Exhibition on Biomass for energy and industry, Seville, 1999.

[3] Henriksen, U., Ahrenfeldt, J., Gøbel, B., Hindsgaul, C. and Jensen, T. K., *The Viking gasifier*, In: Proceedings of the IEA-meeting, London, 2003.

[4] Vijeu, R. and Tazerout, M., *Modélisation et dimensionnement d'une zone de pyrolyse d'un gazogène co-courant*, In: Proceedings of COFRET'04, Nancy, 2004.

[5] Gøbel, B., *Dynamisk modellering af forgasning i fixed koksbed*, Ph.D. Thesis. ET-PHD-99-04, DTU, 1999.

[6] Gøbel, B., Bentzen, J., Hindsgaul, C., Henriksen, U., Ahrenfeldt, J., Fock, F., Houbak N and Qvale, B., *High Performance Gasification with the Two-Stage Gasifier,* In proceedings of 12th European Conference and Technology Exhibition on Biomass for Energy, Industry and Climate Protection. Amsterdam 2002, 389-395.

[7] Milne, T. Abatzoglou N. and Evans, R. J., *Biomass Gasifier "TARS": Their nature, formation and conversion*, report NREL/TP-570-25357, IEA Bioenergy Biomass Utilisation, 1998

[8] Lopez-Matencio, J. L., Bellettre, J. and Lallemand, A., *Numerical prediction of turbulent heat and mass transfer above a porous wall subjected to vaporisation cooling*, I. J. Transport Phenomena, 2003;5(3);185-201.

[9] Jess, A., *Mechanisms and kinetics of thermal reactions of aromatic hydrocarbons from pyrolysis of solid fuels*. Fuel 1996;75(12);1441-1448.

[10] Morf, P., Hasler, P. and Nussbaumer, T., *Mechanisms and kinetics of homogeneous secondary reactions of tar from continuous pyrolysis of wood chips*, Fuel 2002;81(7);843-853.

[11] Jess, A., *Reaktionskinetische Untersuchungen zur thermischen Zersetzung von Modellkohlenwasserstoffen*, Erdöl Erdgas Kohle 1995;111(11);479-484.

[12] Magnussen, B. F., *On the structure of turbulence and a generalised eddy dissipation concept for chemical reaction in turbulent flow*, In: Proceedings of the Nineteenth AIAA Meeting, St Louis, 1981.

[13] Bellettre, J. and Tazerout M., *Numerical simulation of reactive flows in a wood gasifier*, In: Proceedings of the Third Mediterranean Combustion Congress, Marrakech, 2003.

[14] Chui, E. H. and Raithby, G. D., *Computation of radiant heat transfer on a non-orthogonal mesh using the finite-volume method*, Numerical Heat Transfer 1993;23;269-288.

[15] Smith, T. F. Shen Z. F. and Friedman J. N., *Evaluation of coefficients for the Weighted Sum of Gray Gas model*, J. Heat Transfer 1982;104;602-608.

[16] Patankar S. V., *Numerical Heat Transfer and Fluid Flow*, Hemisphere, Washington D.C., 1980.

[17] Ferzieger J. L. and Peric M., *Computational Methods for Fluid Dynamics*, Spinger-Verlag, Heidelberg, 1996.

[18] Bellettre, J., Bataille, F. and Lallemand, A., *A new approach for the study of the turbulent boundary layers with blowing*. International Journal of Heat and Mass Transfer, 1999;42(15);2905-2920.

[19] Shin, D. and Choi, S., *The combustion of simulated waste particles in a fixed bed,* Combustion and Flame, 2000;121;167-180.

[20] Jones, W. P. and Lindstedt R. P., *Global reaction schemes for hydrocarbon combustion*, Combustion and Flame, 1998;73;233-249.

[21] Di Blasi, C., *Dynamic behaviour of stratified downdraft gasifiers*, Chemical Engineering Science 2000;55;2931-2944.

[22] Westbrook, C. K. and Dryer, F. L., *Chemical kinetic modeling of hydrocarbon combustion*, Prog. Energy Combust. Sci. 1984(10);1-57.

[23] Tao, F., Golovitchev, V. and Chomiak, J., *A phenomenological model for the prediction of soot formation in diesel spray combustion*, Combustion and Flame, 2004;136(3);270-282.